OPTIMIZATION OF A STIFFENED COMPOSITE CYLINDER UNDER EXTERNAL HYDROSTATIC PRESSURE FOR UNDERWATER VEHICLES

J.S. Kim[1], J.H. Kweon[1]*, J.H. Choi[2]
[1] Department of Aerospace Engineering, Research Center for Aircraft Parts Technology,
[2] Department of Mechanical Engineering, Research Center for Aircraft Parts Technology,
Gyeongsang National University, South Korea
* Corresponding author (jhkweon@gnu.ac.kr)

Keywords: *Optimization, Stiffened composite cylinder, Buckling, External hydrostatic pressure*

1 Introduction

Over the past few decades, the application of composite materials has been extended to various fields. Composite materials are particularly promising for underwater vehicles because the vehicular performance depends on the weight and the light weight is crucial [1]. Most underwater vehicles for deep sea operations are cylindrical because that shape enables them to effectively withstand external hydrostatic pressure by reducing the bending moment. If the cylindrical structure is not thick enough, it can be vulnerable to buckling under hydrostatic pressure because the buckling of a thin shell structure occurs at a stress level that is much lower than the static strength of the material. On the other hand, excessive thickness adds weight and degrades performance. For this reason, buckling is a critical factor that dominates the structural performance of underwater vehicles. Numerous papers have investigated shell buckling under external pressure. Tsouvalis et al. [2] used a finite element method to study the effect of geometric imperfections on the buckling behavior of composite laminated cylinders under external hydrostatic pressure. Graham [3] investigated the use of composites in deep ocean submersibles by analyzing and testing carbon composite pressure hulls. Gettel et al. [4] used a numerical method to verify the buckling strength of cantilevered cylindrical shells subjected to a transverse load at the free edge. Kim et al. [5] used practical design equations and charts to evaluate the buckling strength of geometrically perfect and imperfect cylindrical shells and tanks subjected to axial compression.

In deep sea a vehicle experiences a high level of external pressure that cannot be supported by a simple shell structure; it needs reinforcement with a frame. Most underwater vehicles use a frame-stiffened structure. Because the circumferential stress in the cylinder under external pressure is double the longitudinal stress, the frame is generally placed in circumferential direction. Several papers focus on the buckling of a stiffened composite panel and cylinder under external pressure. Perret et al. [6] used linear and nonlinear analyses to study the global buckling behavior of a composite stiffened panel. Kidane et al. [7] determined the global buckling load of a cross and horizontal grid-stiffened composite cylinder. Yazdani et al. [8] conducted an experimental study on the buckling behavior of thin-walled glass composite-stiffened cylindrical shells.

The high pressure of a stiffened cylinder may cause a local failure, such as matrix cracking in the vicinity of the stiffener before the buckling arises. Accordingly, the buckling and static failure should be considered together in the design optimization. Some researchers have examined the buckling optimization of a stiffened cylinder [9,10]; few have examined the buckling and static failure simultaneously [11].

This paper presents a basic research on the design of filament-wound underwater vehicles, with a focus on the optimization of the helical winding angle and the ratio of the hoop layer to the helical layer of a frame-stiffened composite cylinder. The objective is to maximize the design load for the external pressure. The total weight is fixed for each configuration, and consideration is given to the effects of the buckling and material failure. A microgenetic algorithm for

the optimization is used in conjunction with the commercial finite element program MSC NASTRAN.

2 Optimization Algorithm

A genetic algorithm [12] is a search heuristic for solving optimization problems. It is used for the optimization of many engineering problems because it obviates the need for an explicit relation between the objective function and the constraints [13,14]. Fig. 1 shows the process of a typical genetic algorithm.

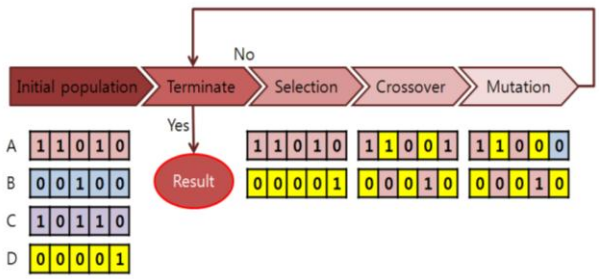

Fig.1. Process of a typical genetic algorithm.

The convergence probability can be increased if the genetic algorithm secures the diversity of the heredity factor by increasing the population size and by using crossover and mutation. Although this method can increase the convergence probability, it also increases the calculation time. The microgenetic algorithm [15] overcomes this problem. It uses nominal convergence and random numbers to make a new generation. Thus, although the microgenetic algorithm has a lower average fitness level than conventional genetic algorithms, it can secure the diversity of a genetic factor with a small population.
Fig. 2 shows the microgenetic optimization algorithm combined with finite element analysis. The genetic information in this study, particularly the helical winding angle and the thickness of the hoop winding, is randomly generated and serves as the initial population. The microgenetic algorithm reads the buckling and failure load from the NASTRAN output file, and the lower value then becomes the design load. The objective is to maximize the design load. Tournament selection [16], which has a short calculation time and uniform crossover [17], is used for optimization. This microgenetic algorithm is based on elitism.

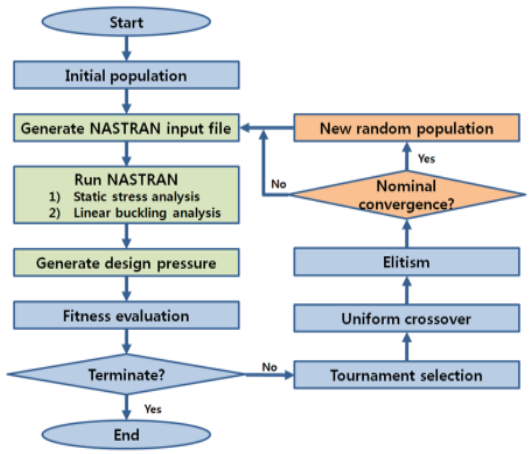

Fig.2. Flowchart of micro genetic algorithm.

The gene with the best fitness in the parent generation survive is compared with the child genes that pass through the selection, crossover and mutation. Nominal convergence is reached if the difference between the parent and child genes is less than a certain threshold, generally 5% [15]; in this situation, an elite gene is generated for the next generation. After the nominal convergence has been reached, the new generation consists of the elite gene from the previous generation and new random genes. The calculation stops at a predefined maximum number of generations.

3 Optimization of a Stiffened Composite Cylinder

3.1 Description of the Problem

Fig. 3 shows the geometry of the stiffened composite cylinder. The cylinders with 0, 1, and 3 frames were analyzed. The geometry was designed to be tested in a further study. In some test chambers [18], the left side of the cylinder is clamped to the equipment wall; thus, no cap is required to cover the cross section.

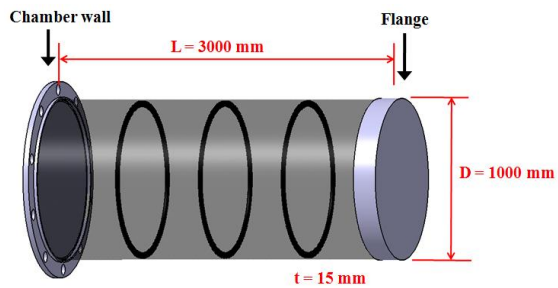

Fig.3. Geometry of cylinder with three frames.

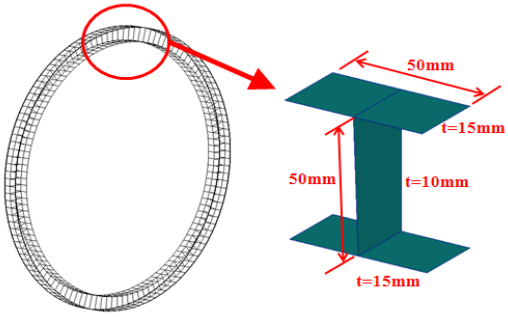

Fig.4. Details of I-frame.

In contrast, the right side needs a strong cap for the application of hydrostatic pressure. A composite I-frame was used for reinforcement in circumferential direction. The mid-plane of the cylinder has a diameter of 1000 mm, a length of 3000 mm, and a thickness is 15 mm. Detail dimensions of the I-frame are shown in Fig. 4.

Fig. 5 shows the finite elements model and boundary conditions. A four-node quadrilateral finite element, CQUAD4 in MSC NASTRAN [19], was used for the modeling of the composite cylinder and frame. A rigid bar element, RBE2 in the same software, was used to idealize the right cap and connect the stiffeners with cylinder. The nodes along the left side of the cylinder are fixed. The nodes on the right edge are clamped and covered with a steel cap. However, they are also subject to longitudinal displacement, which means the cylinder may be deformed in a longitudinal direction.

The applied load is the uniform hydrostatic pressure. For the pressure over the right cap, however, an equivalent concentrated force is applied to the node at center. By using RBE2 element, the nodes along the right edge have a uniform axial displacement.

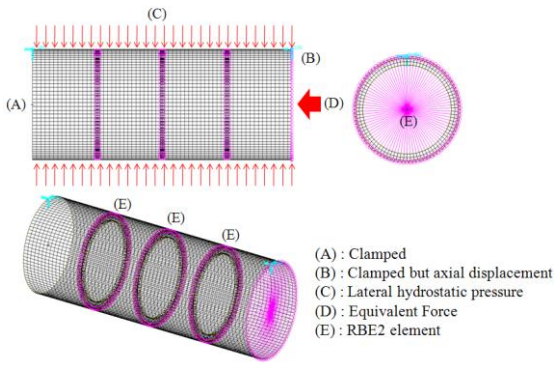

Fig.5. A typical finite element model.

The composite cylinder is assumed to be manufactured by filament winding process and thus consists of helical winding and hoop winding layers as shown in Fig. 6. Twenty-seven layers are considered, including the hoop and helical winding layers. The number of the hoop winding layers is n and the wind angle is 90° (90_n, $0 \le n \le 27$).

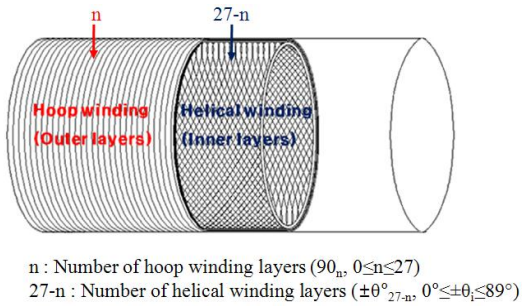

Fig.6. Structure of filament wound cylinder.

Accordingly, the number of helical winding layers is 27-n and the winding angle is θ° ($\pm\theta_{27-n}$, $0^\circ \le \pm\theta_i \le 89^\circ$, where i=27-n). The number of hoop winding layers and the helical winding angle are the design variables.

The material properties given in [18] for the filament wound composite cylinders were used for this study. The effective moduli are used for the frame and the failure of the frame is not considered. The material properties of composite cylinder are E_x = 120.8 GPa, E_y = 8.552 GPa, ν_{xy} = 0.253, G_{xy} = 3.352 GPa, G_{yz} = 2.682 GPa, G_{xz} = 3.352 GPa, X_T = 2064 MPa, Y_T = 32 MPa, and S_{XY} = 45 MPa. The material properties for the frame are E_x = 30.7 GPa, E_y = 65 GPa, ν_{xy} = 0.205, G_{xy} = 15.8 GPa, G_{yz} = 3.13 GPa, and G_{xz} = 2.91 GPa.

The strategy of using a laminated shell element for the filament wound composite cylinder was validated in a comparison with the test results of another paper [18].

3.2 Optimization Results

The optimization parameters for this study are as follows: the population size is 10, the probability of crossover is 0.5, and the nominal convergence is 0.05. The algorithm is based on three assumptions: elitism, tournament selection, and a uniform crossover. The maximum number of generations is 200. Table 1 shows the optimization results for four

examples which have 0, 1, and 3 frames, respectively. All the examples were successfully explored to the global optima, which are exactly the same as the maximum design loads in the feasible region.

Table 1. Results of optimization.

Micro-GA				
	Optimum (MPa)	Helical angle (° deg)	No. hoop layer	Failure mode
Example 1	2.011	75	0	Static
Example 2	2.707	67	0	Buckling
Example 3	4.903	56	0	Buckling
Feasible Region				
	Design Load (MPa)	Helical angle (° deg)	No. hoop layer	Failure mode
Example 1	2.011	75	0	Static
Example 2	2.707	67	0	Buckling
Example 3	4.903	56	0	Buckling

The optimum values of the design load are highly dependent on the number of frames. Regardless of the failure mode, the optimal helical winding angles decrease as the number of frames is increased. This behavior means that a strong frame can carry a greater load in the circumferential direction; it also means there is a decrease in the contribution of the helical winding layers to the load in the hoop direction. The role of the hoop layer in a pressure vessel is to support the stress in the circumferential direction. In frame-reinforced cylinders, however, the frame takes over the role of the hoop layers. Thus, as indicated by the results in Table 1, no additional hoop winding is needed over the helical winding in a stiffened cylinder. Fig. 7 separately shows the optimized design loads which consider the buckling and failure together, the buckling-only loads which are optimized by considering the buckling only, and failure-only loads which are optimized by considering the static failure only.

It should be noted that even though the example 1 fails in static failure mode at the optimization point, the optimized failure load is much lower than the one from the failure-only load. When only the static failure is considered for optimization, the failure-only load is higher than 8 MPa. However, the optimized design load considering the buckling and static failure is about 2.0 MPa which is slightly lower than the buckling-only load.

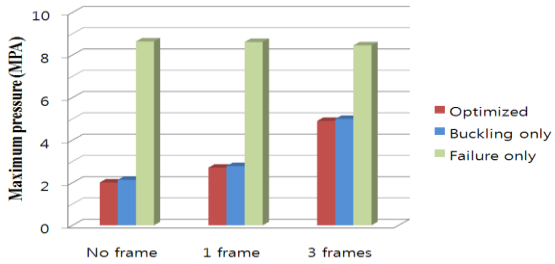

Fig.7. Comparison of optimized design loads and buckling-only and failure-only loads

Similar phenomena are found in example 2 and 3. In the examples, the optimized cylinders show the buckling. However, the optimized buckling loads are slightly lower than the buckling-only loads. It means that the cylinders fail in static failure mode at the optimal points when only the buckling is considered. The buckling loads should always be interpreted in conjunction with the buckling mode shapes. Fig. 8 shows the buckling modes. In the no frame cylinder, when the buckling occurs, three waves are formed along the circumference and a long wave is formed in the longitudinal direction. The shape of the buckling mode is much different in each of the cylinders with frames (examples 2 and 3). Clearly, the buckling modes are greatly affected by the frames. The number of longitudinal waves is determined by the number of frames.

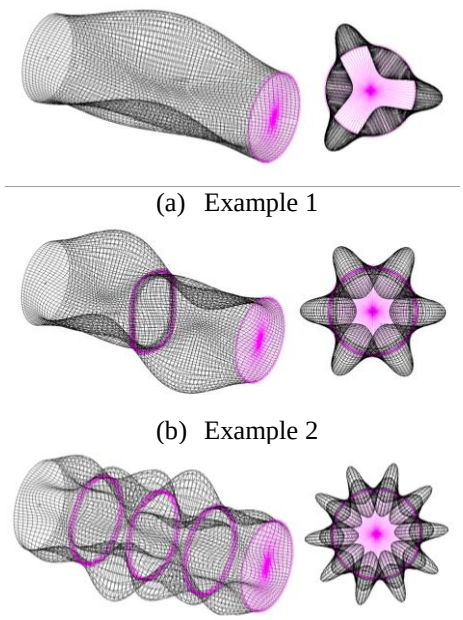

(a) Example 1

(b) Example 2

(c) Example 3

Fig.8. Buckling modes at optimum.

Complicated buckling modes generally lead to higher buckling loads. This principle is confirmed through the relation between the buckling loads and buckling modes in the examples. An increase in the buckling load can induce local compressive failures before the onset of buckling. That is why the optimized design load, which is determined from the buckling, is different from the buckling-only load.
Fig. 9 shows the points which the microgenetic algorithm explored to search an optimum point over the feasible region of example 2. The figure shows that the calculation points are concentrated around the optimal point.

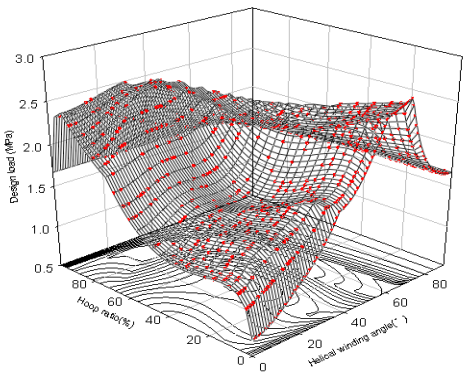

Fig.9. Calculation points for the optimization of no-frame cylinder (example 2)

3.3 Feasible Region

As shown in Fig. 10, the accuracy of the optimization process was verified by examining the feasible regions of the examples. Each figure has two feasible surfaces: one for a static failure load and one for a buckling load. There were 2403 analysis points. The fringe on the bottom plane shows the design loads at every hoop winding ratio and helical winding angle.
In the example 1 (which has no stiffener), the buckling load surface dominates the structural performance of cylindrical structures. At a 75° of helical winding angle and a zero hoop winding ratio, however, the static failure load becomes slightly lower than the buckling load and it determined the global optimum. Because a frame around the circumference is reinforced in example 2, two feasible surfaces overlap each other near the range of a 70° helical winding angle and a zero hoop winding ratio.

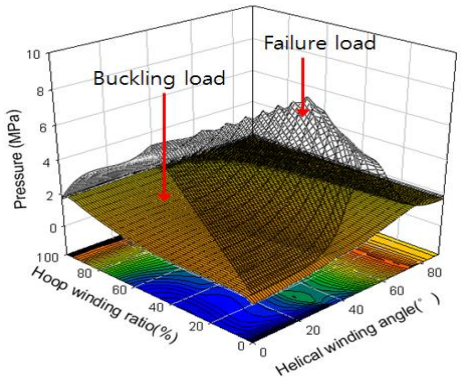

(a) Example 1

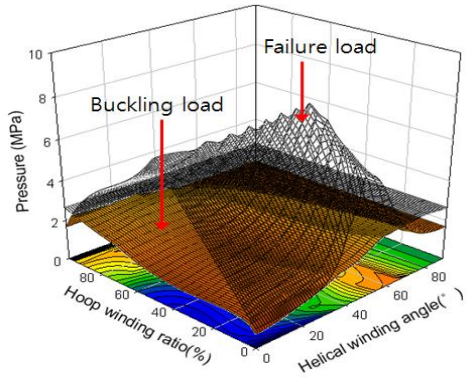

(b) Example 2

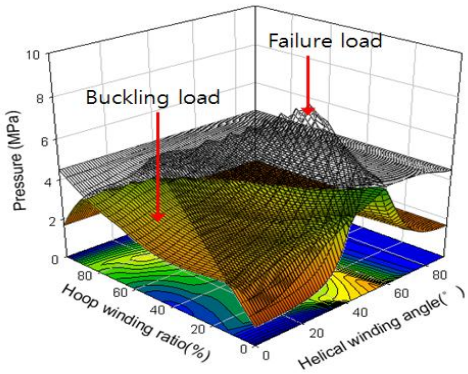

(c) Example 3
Fig.10. Feasible region

When three frames are stiffened in example 3, the overlapped region becomes much complicated in the range of a 60° helical winding angle and a zero hoop winding ratio.

4 Conclusion

This basic research shows how the application of composite materials to underwater vehicles can be optimized by the helical winding angle and the hoop

winding ratio of a stiffened composite cylinder under hydrostatic pressure. The design variables are the helical winding angle and the hoop winding ratio, and the objective is to maximize the design load. The buckling load and static failure were both considered. The adapted micro genetic algorithm successfully found the global optimum of all the considered examples.

The optimized results of the stiffened composite cylinders provide interesting information. They show that, regardless of the failure mode, the optimal helical winding direction moves far from the hoop direction as the number of frames increases. The results also confirm that, in the frame-reinforced cylinders, the frame takes over the role of the hoop layers, obviating the need for an additional hoop winding layer over the helical winding layers.

References

[1] C.T.F. Ross "A conceptual design of an underwater vehicle". *Ocean Engineering*, Vol. 33, No. 16, pp 2087-2104, 2006.

[2] N.G Tsouvalis, A.A Zafeiratou and V.J Papazoglou "The effect of geometric imperfections on the buckling behaviour of composite laminated cylinders under external hydrostatic pressure". *Composites Part B: Engineering*, Vol. 34, No. 3, pp 217-226, 2003

[3] D. Graham "Composite pressure hulls for deep ocean submersibles". *Composite Structures*, Vol. 32, pp 331-343, 1995

[4] M. Gettel and W. Schneider "Buckling strength verification of cantilevered cylindrical shells subjected to transverse load using Eurocode 3". *Journal of Constructional Steel Research*, Vol. 63, No. 11, pp 1467-1478, 2007

[5] S.E. Kim and C.S. Kim "Buckling strength of the cylindrical shell and tank subjected to axially compressive loads". *Thin-Walled Structures*, Vol. 40, No. 4, pp 329-353, 2002

[6] A. Perret, S. Mistou and M. Fazzini "Global behaviour of a composite stiffened panel in buckling. Part 1: Numerical modeling". *Composite Structures*, Available online 4 may 2011

[7] S. Kidane, G. Li, J. Helms, S.S. Pang and E. Woldesenbet "Buckling load analysis of grid stiffened composite cylinders". *Composites Part B: Engineering*, Vol. 34, No. 3, pp 1-9, 2003

[8] M. Yazdani and G. H. Rahimi "The effects of helical ribs' number and grid types on the buckling of thin-walled GFRP-stiffened shells under axial loading". *Journal of Reinforced Plastics and Composites*, Vol. 29, No. 17, pp 2568-2575, 2010

[9] Y.D. Seo, S.K. Youn, J.H. Yeon, S.Y. Chang and J.T. Yoo "Topology optimization of inner-wall stiffener for critical buckling loads of cylindrical containers". *Transactions of the KSME A*, Vol. 29, No. 3, pp 503-510, 2005

[10] G. Sun and R. Mao "Optimization of stiffened laminated-composite circular-cylindrical shells for buckling". *Composite Structures*, Vol. 23, No. 1, pp 53-60, 1993

[11] N. Jaunky, N.F. Knight Jr and D.R. Ambur "Optimal design of general stiffened composite circular cylinders for global buckling with strength constraints". *Composite Structures*, Vol. 41, No. 3-4, pp 243-252, 1988

[12] D.E. Goldberg "*Genetic algorithm in search, optimization and machine learning*". 1st edition, Addison-Wesley Professional, 1989

[13] G. Louis, T.G. Maxime and M.P. François "Review of utilization of genetic algorithms in heat transfer problems". *International Journal of Heat and Mass Transfer*, Vol. 52, No. 9-10, pp 2169-2188, 2009

[14] S.F. Hwanga and R.S. Hea "Improving real-parameter genetic algorithm with simulated annealing for engineering problems". *Advances in Engineering Software*, Vol. 37, No. 6, pp 406-418, 2006

[15] K. Krishnakumar "Micro-genetic algorithms for stationary and non-stationary function optimization". *Proceedings of the SPIE*, Germany, Vol. 1196, pp 289-296, 1990

[16] B.L. Miller and D.E. Goldberg "Genetic algorithm tournament selection and the effect of noise". *Complex Systems*, Vol. 9, pp 193-212, 1995

[17] G. Syswerda "Uniform crossover in genetic algorithm". *Proc. of the 3rd Int. Conf. on Genetic Algorithms*, San Francisco, pp 2-9, 1989

[18] MSC.NASTRAN User's Guide.

[19] C.J. Moon, I.H. Kim, B.H. Choi, J.H. Kweon and J.H. Choi "Buckling of filament-wound composite cylinders subjected to hydrostatic pressure for underwater vehicle applications". *Composite Structures*, Vol. 92, No. 9, pp 2241-2251, 2010.

Acknowledgement

This work was supported by the Underwater Vehicle Research Center of the Agency for Defense Development and Priority Research Centers Program through the National Research Foundation of Korea(NRF) funded by the Ministry of Education, Science and Technology(2010-0029689).